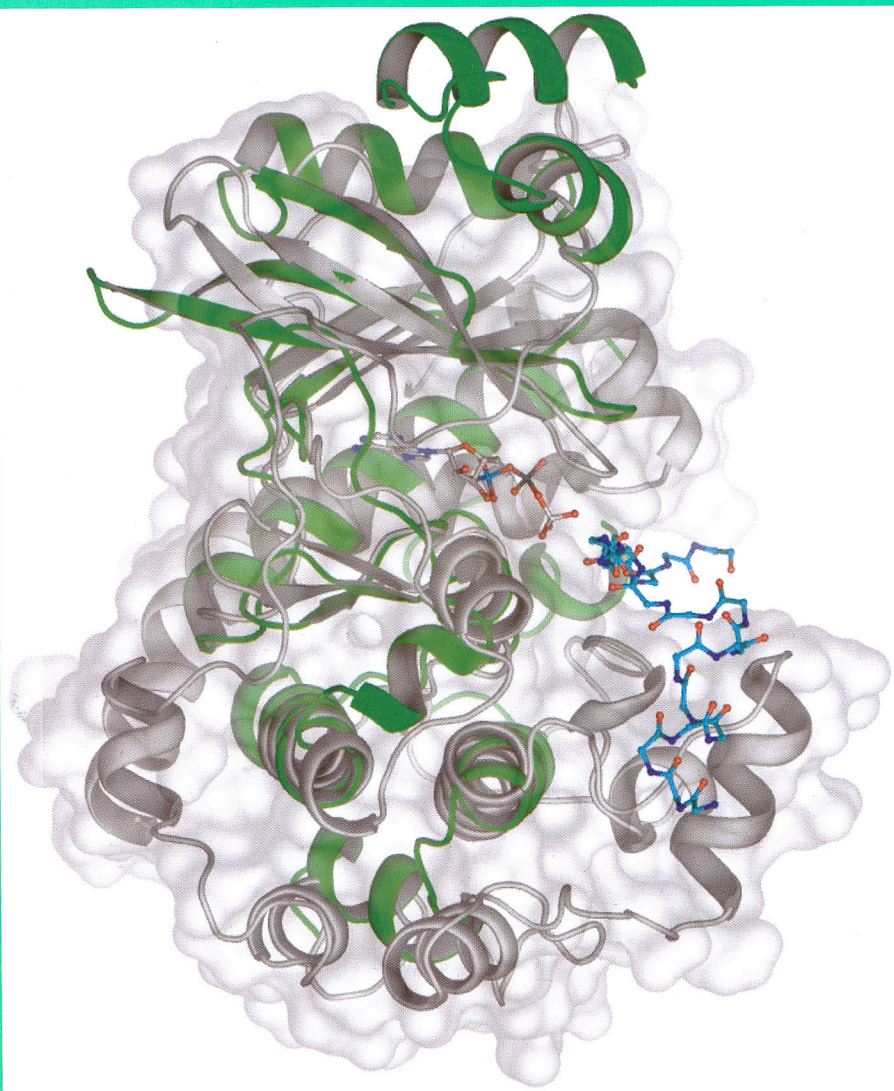




www.febsjournal.org

the FEBS Journal

Volume 272 Number 14 July 2005



Review Article

cAMP and signalling
pathways

Hypothesis

Death inducer obliterator
protein



Blackwell
Publishing

Structure and activity of the atypical serine kinase Rio1

Nicole LaRonde-LeBlanc¹, Tad Guszczynski², Terry Copeland² and Alexander Wlodawer¹

¹ Protein Structure Section, Macromolecular Crystallography Laboratory, National Cancer Institute, NCI-Frederick, MD, USA

² Laboratory of Protein Dynamics and Signaling, National Cancer Institute, NCI-Frederick, MD, USA

Keywords

autophosphorylation; nucleotide complex; protein kinase; ribosome biogenesis; Rio1

Correspondence

A. Wlodawer, National Cancer Institute, MCL, Bldg. 536, Rm. 5, Frederick, MD 21702-1201, USA
Fax: +1 301 8466322
Tel: +1 301 8465036
E-mail: wlodawer@ncifcrf.gov

(Received 21 April 2005, revised 24 May 2005, accepted 27 May 2005)

doi:10.1111/j.1742-4658.2005.04796.x

Rio1 is the founding member of the RIO family of atypical serine kinases that are universally present in all organisms from archaea to mammals. Activity of Rio1 was shown to be absolutely essential in *Saccharomyces cerevisiae* for the processing of 18S ribosomal RNA, as well as for proper cell cycle progression and chromosome maintenance. We determined high-resolution crystal structures of *Archaeoglobus fulgidus* Rio1 in the presence and absence of bound nucleotides. Crystallization of Rio1 in the presence of ATP or ADP and manganese ions demonstrated major conformational changes in the active site, compared with the uncomplexed protein. Comparisons of the structure of Rio1 with the previously determined structure of the Rio2 kinase defined the minimal RIO domain and the distinct features of the RIO subfamilies. We report here that Ser108 represents the sole autophosphorylation site of *A. fulgidus* Rio1 and have therefore established its putative peptide substrate. In addition, we show that a mutant enzyme that cannot be autophosphorylated can still phosphorylate an inactive form of Rio1, as well as a number of typical kinase substrates.

Ribosome biogenesis is fundamental to cell growth and proliferation and thereby to tumorigenesis. It has been shown that ribosome biogenesis and cell cycle progression are tightly linked through a number of mechanisms [1,2]. Not surprisingly, several oncogenes have been shown to deregulate ribosome biogenesis, in order to meet the demand for cell growth and increased protein production [3]. For example, increased levels of ribosome biogenesis have been reported for human breast cancer cells with decreased pRb and p53 activity [4]. Ongoing studies in yeast have identified many of the nonribosomal factors necessary for the proper processing of ribosomal RNA (rRNA) [5]. More recent efforts using proteomics methods have begun to pinpoint the protein factors required for this critical process. Although many of the factors have been identified, the specific roles they play in rRNA processing or ribosomal subunit assembly have not been clarified. Understanding these basic pathways on a molecular level is important for providing insight into how the connection between ribosome biogenesis

and cell cycle control might be used to our advantage, such as design of new classes of drugs.

Protein kinases are known players in the regulation of cell cycle control, in addition to their role in a wide variety of cellular processes including transcription, DNA replication, and metabolic functions. This large protein superfamily contains over 500 members in the human genome [6] and represents one of the largest protein superfamilies in eukaryotes [7]. One major class of eukaryotic protein kinases (ePKs) catalyzes phosphorylation of serine or threonine, while another one phosphorylates tyrosine residues [8–10]. All these enzymes contain catalytic domains composed of conserved secondary structure elements and catalytically important sequences referred to as ‘subdomains’ that create two globular ‘lobes’ linked by a flexible ‘hinge’ [7,8,10]. Twelve subdomains are recognized in ePKs: I to IV comprising the N-terminal lobe, V producing the hinge, and VIa, VIb, and VII to XI forming the C-terminal lobe. The three-dimensional structure of the ePK kinase domain is well established and the

Abbreviations

aPK, atypical protein kinase; ePK, eukaryotic protein kinase; MAD, multiwavelength anomalous diffraction; N-lobe, N-terminal kinase lobe; RMSD, root mean square deviation.

conserved subdomain residues have been shown to be involved in phosphotransfer, as well as in recognition and binding of ATP or substrate peptides [8,9,11,12].

Several protein subfamilies have been identified that are not significantly related to ePKs in sequence but contain a 'kinase signature' [6]. Based on the presence of these limited sequence motifs and/or demonstrated kinase activity, these proteins have been collectively named atypical protein kinases (aPKs) [6]. Unlike ePKs, aPK families are small, typically containing only a few (1–6) members per organism [6]. The RIO protein family has been classified as aPK based on demonstrated kinase activity of the yeast Rio1p and Rio2p and on the identification of a conserved kinase signature, although these enzymes exhibit no significant homology to ePKs [6]. The RIO family is the only aPK family conserved in archaea, and it has been suggested that this family represents an evolutionary link between prokaryotic lipid kinases and ePKs [13].

The founding member of the RIO kinase family is Rio1p, an essential gene product in *Saccharomyces cerevisiae* that functions as a nonribosomal factor necessary for late 18S rRNA processing [14,15]. Depletion of Rio1p results in accumulation of 20S pre-rRNA, cell cycle arrest, and aberrant chromosome maintenance [14,16]. Sequence alignments have demonstrated that members of two RIO subfamilies, Rio1 and Rio2, are represented in organisms from archaea to mammals [13,17,18], whereas a third subfamily, Rio3, is found strictly in higher eukaryotes. The RIO kinase domain is generally conserved among the three subfamilies, but with distinct differences. In addition, the Rio2 and Rio3 subfamilies are characterized by conserved N-terminal domains outside of the RIO domain that are unique to each of the two subfamilies and are not present in Rio1. Yeast contains one Rio1 and one Rio2 protein, but no members of the Rio3 subfamily. Depletion of yeast Rio2 also affects growth rate and results in an accumulation of 20S pre-rRNA [18,19]. Therefore, both RIO proteins are critically important for ribosome biogenesis. Although there is significant sequence similarity between Rio1 and Rio2 proteins (43% similarity between the yeast enzymes), Rio1 proteins are functionally distinct from Rio2 proteins and do not complement their activity, as deletion of Rio2 in yeast is also lethal, despite functional Rio1 [19].

Yeast RIO proteins are capable of serine phosphorylation *in vitro*, and residues equivalent to the conserved catalytic residues of ePKs are required for their *in vivo* function [15–18]. Our recently reported crystal structure of Rio2 from *Archaeoglobus fulgidus* has demonstrated that the RIO domain resembles a trimmed version of an ePK kinase domain [20]. It consists of

two lobes which sandwich ATP and contains the catalytic loop, the metal-binding loop, and the nucleotide-binding loop (P-loop, glycine-rich loop), but lacks the classical substrate-binding and activation loops (subdomains VIII, X and XI) present in ePKs. The structure also revealed that the conserved Rio2-specific domain contains a winged helix motif, usually found in DNA-binding proteins, tightly connected through extensive interdomain contacts to the RIO kinase domain. An entire 18 amino acid loop in the N-terminal kinase lobe (N-lobe) of Rio2, containing several subfamily specific conserved residues, was not observed in the crystal structure due to its flexibility. Differences between the sequences of the Rio1 and Rio2 kinases in several key regions of the RIO domain have led us to the conclusion that structural differences may exist between them which could explain their distinct functionality and separate conservation.

To investigate the functional distinction of Rio1 and its relationship to Rio2, we have solved several X-ray crystal structures of Rio1 from *A. fulgidus* (AfRio1), with and without bound nucleotides. Crystallization of Rio1 protein in the presence of ATP and manganese demonstrated partial hydrolysis of ATP, consistent with data that indicate much higher autophosphorylation activity of Rio1 than Rio2. We have also shown that Rio1 is active in phosphorylating several kinase substrates and characterized its autophosphorylation site. Analysis of the data reported here allowed us to identify the key differences between Rio1 and Rio2 proteins and highlighted the unique features of RIO proteins in general.

Results

Structure determination and the overall fold of AfRio1

Full-length Rio1 from the thermophilic organism *A. fulgidus* was expressed in *Escherichia coli* in the presence of selenomethionine (Se-Met). The enzyme was purified using heat denaturation (in order to denature *E. coli* proteins while leaving the thermostable Rio1 protein intact), affinity chromatography, and size-exclusion chromatography. Mass spectrometry confirmed that the purified protein contained all the expected residues (1–258). We obtained two substantially different crystal forms of AfRio1. Crystals grown without explicit addition of ATP or its analogs belong to the space group P2₁, contain one molecule per asymmetric unit, and diffract to the resolution better than 2.0 Å. The structure was solved using the multiwavelength anomalous diffraction (MAD) phasing technique

with Se-Met substituted protein at 1.9 Å. The model contains residues 6–257 of the 258 residues of AfRio1, with both termini being flexible. Crystals grown in the presence of adenosine-5'-triphosphate (ATP) or adenosine-5'-diphosphate (ADP) and Mn²⁺ ions also belong to the space group P2₁, but are quite distinct, containing four molecules in the asymmetric unit. Manganese ions were used in the place of magnesium ions for better detection in electron density maps, and have been shown to support catalysis *in vitro* with this enzyme (data not shown). The nucleotide-complex structures were solved by molecular replacement, using the coordinates described above as the search model. Data collection and crystallographic refinement statistics for both crystal forms are shown in Table 1.

The determination of the structure of Rio1 and the availability of the previously determined structure of Rio2, has enabled us to define the minimal consensus RIO domain (Fig. 1A). Similar to ePKs, it consists of an N-lobe comprised of a twisted β-sheet (β1–β6) and a long α-helix (αC) that closes the back of the ATP-binding pocket, a hinge region, and a C-lobe which forms the platform for the metal-binding loop and the catalytic loop. However, the RIO kinase domain contains only three of the canonical ePK α-helices (αE, αF, and αI) in the C-lobe. In both Rio1 and Rio2, an additional α-helix (αR), located N-terminal to the canonical N-lobe β-sheet, extends the RIO domain (Figs 1A and 2A). All RIO domains also contain an insertion of 18–27 amino acids between αC and β3. In the Rio1 structure solved from data obtained using

crystals grown in the absence of ATP (APO-Rio1), we were able to trace that part of the chain in its entirety (Figs 1A and 2A). In the structures of AfRio2, however, no electron density was observed for most of this region, and thus we have called it the 'flexible loop' (Fig. 1B). The overall fold of the kinase domain of Rio1 is very homologous to that of the Rio2, but significant local differences between the two proteins result in root mean square deviation (RMSD) of 1.39 Å (for 217 Cα pairs of complexes with ATP and Mn²⁺ ions). Comparison of the Rio1 structure with that of c-AMP-dependent protein kinase (PKA) showed that like Rio2, Rio1 lacks the activation or 'APE' loop (subdomain VIII) and subdomains X and XI seen in canonical ePKs (Fig. 1C). In addition to the N-terminal α-helix specific to RIO domain, Rio1 contains another two α-helices N-terminal to the RIO domain, as opposed to the complete winged helix domain present in Rio2 (Fig. 1A,B).

Although no nucleotide was added to the protein used for the determination of the APO-Rio1 structure, electron density in which we could model an adenosine molecule was observed in the active site. However, no density which would correspond to any part of a triphosphate group was seen. The bound molecule (Fig. 1A) must have remained complexed to the enzyme through all steps of purification of the Rio1 protein, which is quite remarkable as two affinity column purification steps and one size-exclusion column purification step were performed. As such, this molecule must bind to Rio1 with extremely high affinity,

Table 1. Data collection and refinement statistics for the APO, ATP- and ADP-bound Rio1.

| Crystal data | Se-Met MAD | | | | |
|---------------------------------|---------------|---------------|---------------|---------------|---------------|
| | Peak | Edge | Remote | ATP-Mn | ADP-Mn |
| Space group P2 ₁ | | | | | |
| a (Å) | | 42.99 | | 53.31 | 53.41 |
| b (Å) | | 52.70 | | 80.37 | 80.08 |
| c (Å) | | 63.78 | | 121.32 | 121.06 |
| β (°) | | 108.89 | | 90.02 | 90.17 |
| λ (Å) | 0.97947 | 0.97934 | 0.99997 | 0.96860 | 0.96860 |
| Resolution (Å) | 40–1.90 | 40–2.10 | 40–1.99 | 30–2.00 | 30–1.89 |
| R _{sym} (last shell) | 0.075 (0.259) | 0.085 (0.283) | 0.066 (0.233) | 0.106 (0.286) | 0.147 (0.350) |
| Reflections | 40612 (3463) | 30503 (2899) | 35301 (3339) | 65296 (5149) | 82669 (6470) |
| Redundancy | 3.6 (2.8) | 3.6 (2.7) | 3.7 (3.1) | 3.8 (3.7) | 7.5 (6.8) |
| Completeness (%) | 97.6 (83.5) | 98.8 (93.0) | 98.5 (83.5) | 90.1 (71.4) | 94.2 (74.1) |
| R/R _{free} (%) | | 15.9/24.7 | 17.7/24.9 | 18.9/26.3 | |
| (Last shell) | | | | | |
| Mean B factor (Å ²) | | | 31.20 | 23.42 | 30.51 |
| Residues | | | 253 | 980 | 980 |
| Waters | | | 275 | 921 | 831 |
| RMS Deviations | | | | | |
| Lengths (Å) | | | 0.032 | 0.018 | 0.016 |
| Angles (°) | | | 2.29 | 1.68 | 1.60 |

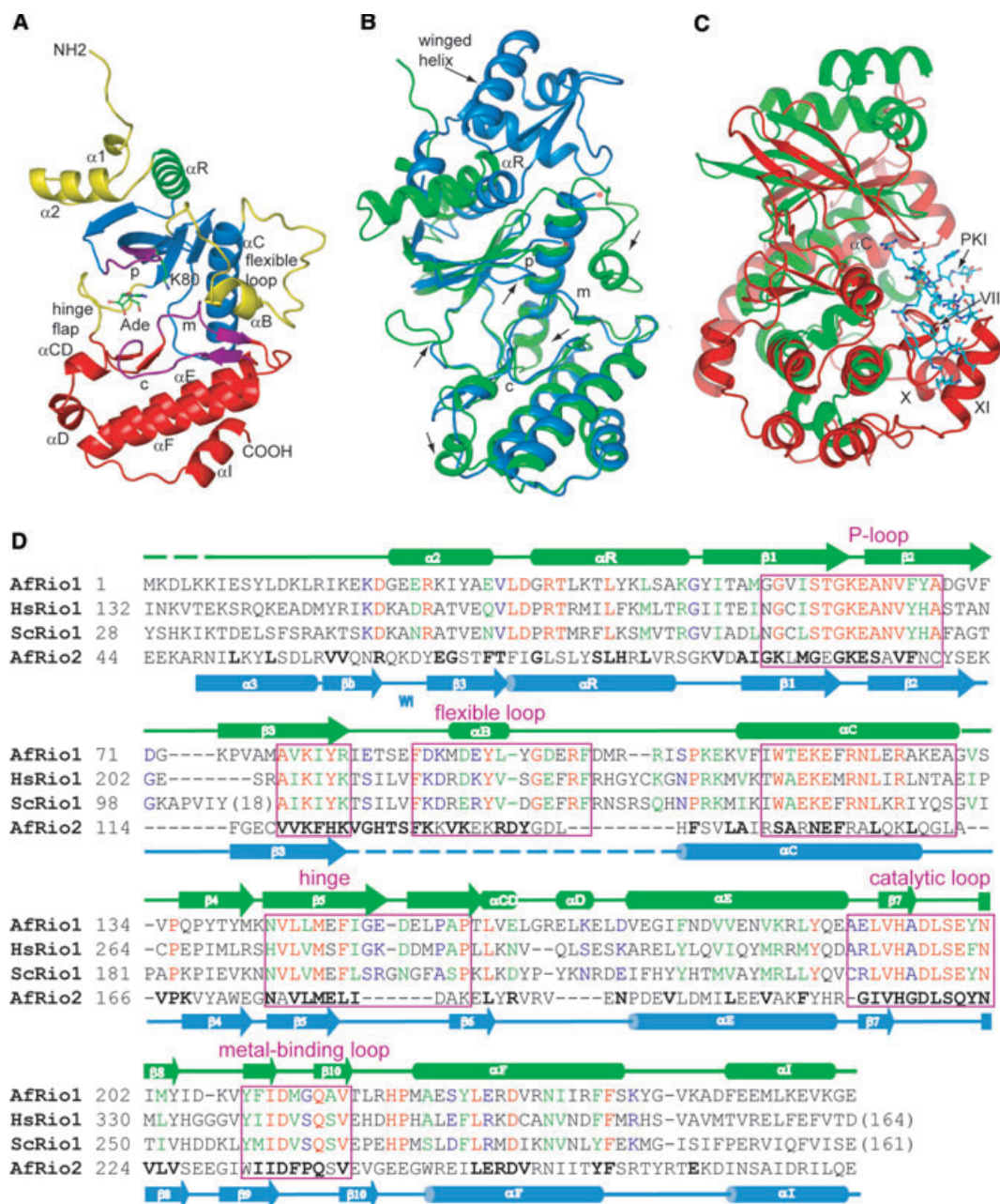


Fig. 1. The structure and conservation of Rio1. (A) The structure of APO-Rio1 showing the important kinase domain features and the Rio1-specific loops (yellow). The P-loop, metal-binding loop and catalytic loop are indicated in all figures by p, m and c, respectively (purple). (B) An alignment of the polypeptide chains of the ATP-Mn complexes AfRio1 (green) with AfRio2 (blue; PDB code 1ZAO). Arrows indicate significant differences in structure between the two molecules. The position of αR and the winged helix of Rio2 is also indicated. (C) An alignment of the Rio2-ATP-Mn complex (green) with the PKA-ATP-Mn-peptide inhibitor complex (red; PDB code 1ATP). The peptide inhibitor is shown in cyan stick representation (PKI), and the subdomains of PKA molecule absent in Rio1 are labeled. (D) Sequence alignment of AfRio1 with the enzymes from (*H. sapiens* and *S. cerevisiae*), as well as with AfRio2. Rio1 sequences are colored red for identical, green for highly similar, and blue for weakly similar residues as calculated by CLUSTALW using the sequences shown as well as those from *Caenorhabditis elegans*, *Drosophila melanogaster* and *Xenopus laevis*. The AfRio2 sequence is structurally aligned to the AfRio1 and is bolded for residues that are identical or highly similar among Rio2 proteins. The elements of secondary structure of the *Archaeoglobus* enzymes are shown above and below the alignments, with colors corresponding to (B).

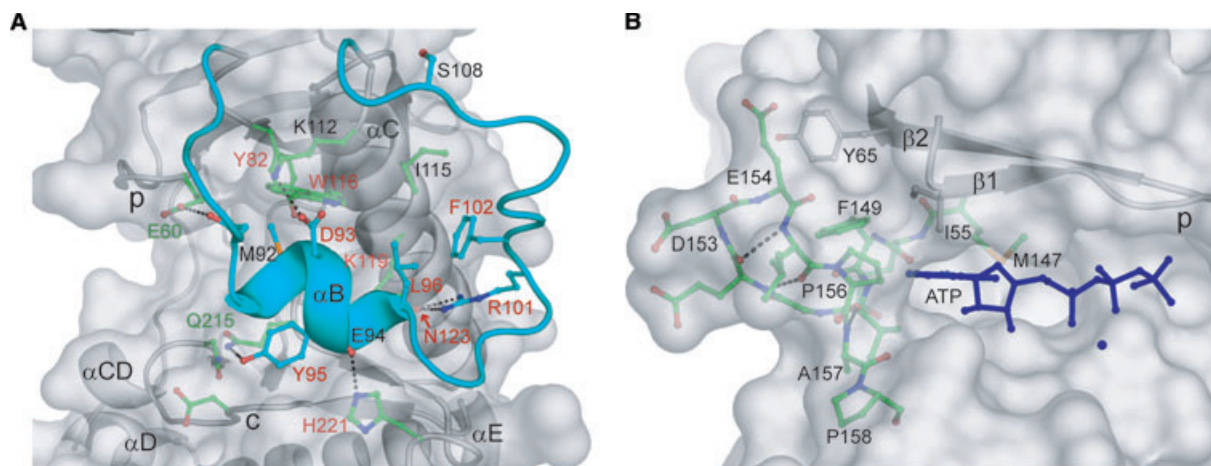


Fig. 2. The flexible loop and flap of Rio1. (A) The flexible loop of Rio1 showing the interactions between the loop and the rest of the proteins. The loop is colored in cyan, residues that are involved in the interaction are shown in stick representation. Rio1-conserved residues are labeled in red text. Those residues that are also conserved in Rio2 proteins are indicated in green text. (B) The structure of the flap in the hinge region. Residues of the hinge region are shown in green stick representation.

and the model presented here does not represent a true APO form. However, the structure in the absence of added nucleotide does not represent an ATP-bound form either. When nucleotide is added, Rio1 undergoes conformational changes that result in a new crystal form. Comparison of the APO and nucleotide-bound structures indicates that in the presence of ATP or ADP, two portions of the flexible loop become disordered, and that the part that remains ordered changes conformation and position relative to the rest of Rio1 molecule (Fig. 3A,B). In addition, the catalytic loop and the metal-binding loop both move significantly when ATP is added (Fig. 3A,B). The overall RMSD between the two states is 0.91 Å for 228 C α pairs. The γ -phosphate is modeled with partial occupancy, as high temperature factors suggested that a fraction of the molecules were hydrolyzed. Comparisons of the four crystallographically independent molecules in the Rio1-ATP complex showed that the N-terminal Rio1-specific helices and α D adopt different positions, and two of the molecules show a slightly different positioning of the ATP γ -phosphate relative to the other two (Fig. 3C). The structures of the Rio1-ATP-Mn and the Rio1-ADP-Mn complexes are virtually identical, indicating that the conformational changes which occur require neither the presence of the γ -phosphate nor autophosphorylation (Fig. 4A).

The flexible loop and hinge region of the Rio1 kinases

The loop between α C and β 3 of the RIO kinase domain shows distinct conservation in each RIO

subfamily (Fig. 1D). In the case of Rio2, the electron density for that region was not observed in any crystals that have been studied to date. However, the sequence in this region is highly conserved, suggesting that it plays an important role in the function of Rio2 kinases. Similarly, Rio1 kinases also exhibit significant conservation of residues in this loop (Fig. 1D). Alignment of *A. fulgidus* and *S. cerevisiae* Rio1 with human, zebrafish, dog, plant, fly, and worm homologs yields 60% similarity and 20% identity in the sequence in this region (data not shown). This increases to 87.5% similarity and 66% identity when the yeast and archaeal sequences are omitted from the alignment. In the structure of APO-Rio1 presented here, this loop consists of 27 amino acids (Arg83 of β 3 through Glu111 of α C) and is significantly longer than the 18 amino acids long disordered loop of Rio2 (Fig. 1D). In the APO-Rio1 structure, this loop starts with a poorly ordered chain between residues 84 and 90. This region is characterized by weak density and high temperature factors and makes no direct contact with other parts of the protein, thus none of the side chains were modeled (Fig. 2A). Residues 90–96 form a small α -helix, followed by a β -turn between Leu96 and Asp99. Three more β -turns follow between Asp99 and Phe102, Met104 and Ile107, and Ser108 and Glu111, which marks the start of α C. The entire flexible loop packs between the N-terminal portion of α C and part of the C-lobe (Figs 2A and 3A).

The interactions between the flexible loop and the rest of the protein include several hydrogen bonds between conserved residues (Fig. 2A). The side chain of Asp93 makes a hydrogen bond to Lys112, which is

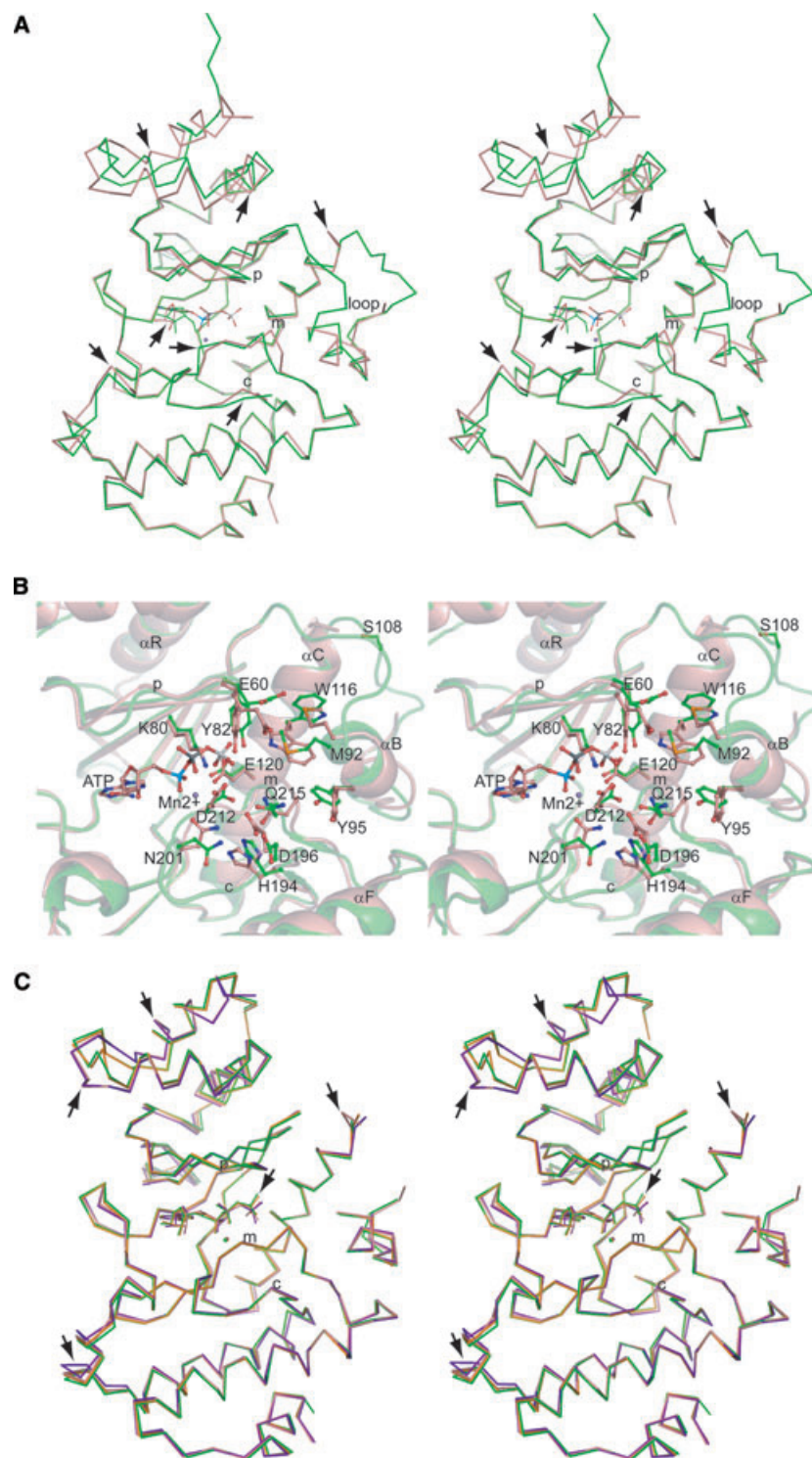


Fig. 3. Conformational changes upon binding to nucleotide. (A) Stereoview of the overall alignment of APO-Rio1 (green) and Rio1-ATP-Mn complex (chain A; pink). (B) Close-up alignment of the APO-Rio1 and Rio1-ATP-Mn complex including the catalytic, metal-binding, and flexible loops. (C) The alignment of the four molecules in the asymmetric unit of the crystals of Rio1-ATP-Mn.

replaced by a methionine in other Rio1 sequences. This interaction is absent when nucleotide is added. Tyr95 and Gln215 interact via a hydrogen bond which is lost in the presence of nucleotide, when Gln215 interacts with the backbone carbonyl of the metal-binding

Asp212 to stabilize its position. In this case, Tyr95 forms instead a hydrogen bond with Arg230. Arg101 and Asn123 interact via hydrogen bond to hold the flexible loop in place. The carbonyl oxygen of Glu94, at the C-terminal end of the flexible loop helix, forms

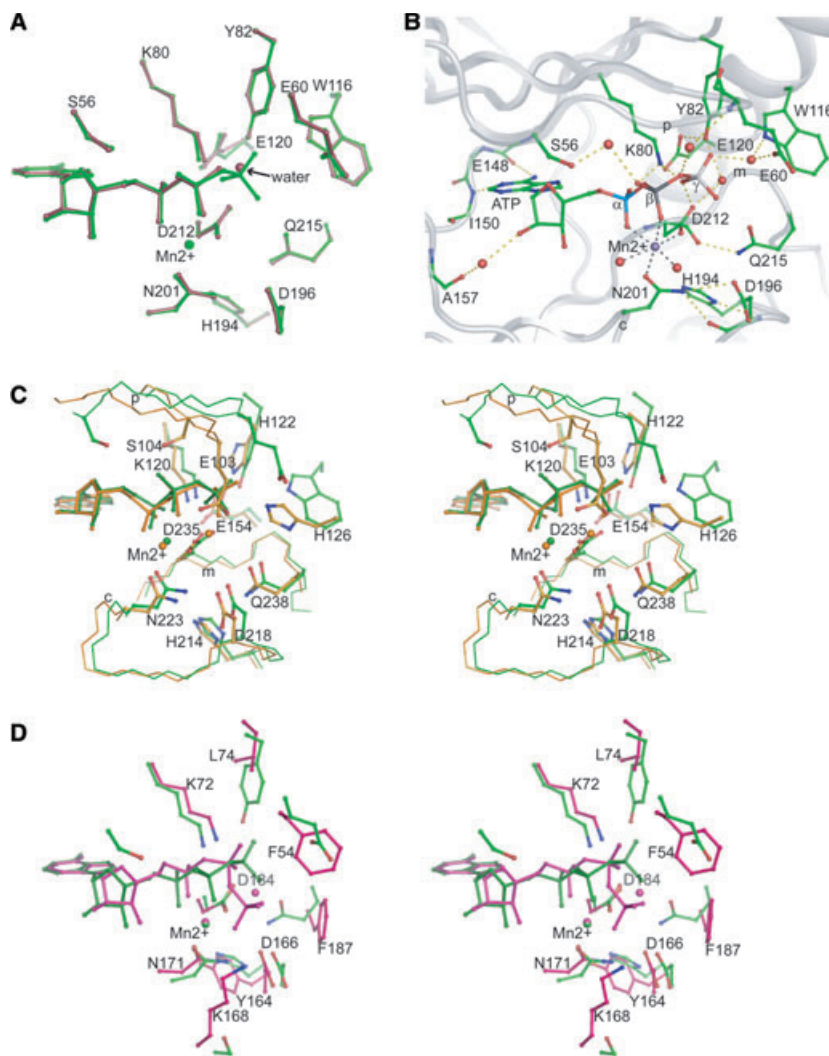


Fig. 4. Nucleotide binding by Rio1. (A) Alignment of the active site residues of the Rio1-ATP-Mn complex (green) on that of the Rio1-ADP-Mn complex (purple). (B) View of ATP bound in the active site of Rio1. Hydrogen bonds are shown as yellow dashed lines, coordinate bonds are shown in black. (C) Stereoview of the alignment of the active sites of AfRio1 (green) and AfRio2 (orange; PDB code 1ZAO). (D) Stereoview of the alignment of the active sites and bound nucleotide of AfRio1 (green) and PKA (magenta; PDB code 1ATP).

a hydrogen bond with His221. In addition to hydrogen bonds, hydrophobic packing of Leu96, Ile115, and Phe102 stabilizes the interactions of the flexible loop with the rest of the protein. Another interesting hydrophobic interaction is observed between Met92 and Trp116 of α C, with both residues packing against each other in the absence and presence of ATP (Fig. 3B). However, their side chains switch positions between the APO and nucleotide-bound state, bringing the tryptophan side chain closer to the active site where it participates in a water-mediated interaction with the γ -phosphate in the ATP-bound form (Figs 3B and 4B). In the presence of ATP or ADP, residues 85–91 and 104–109 are not seen in the electron density, emphasizing the flexibility of this region (Fig. 3A,B).

Another distinguishing feature of the Rio1 kinase domain is a conserved insertion of five residues in the hinge region between the N- and C-lobes which forms

a β -hairpin 'flap' (Ile150 to Ala157) that buries part of the adenine ring of ATP (Fig. 2B). No equivalent feature was seen in the structure of Rio2 or in any other kinase structures that we examined. As a result of the presence of the flap, the adenosine ring of ATP is buried in a deeper pocket in the kinase domain of Rio1 than in Rio2. The flap packs against the rest of the molecule through hydrophobic interactions between Glu154 and Tyr65, as well as between Pro156 and Ile55. Phe149, just N-terminal to the flap, provides further packing surface for Tyr65 (Fig. 2B). No polar contacts are observed between the flap and the ATP, but hydrophobic packing interactions are seen between the adenosine ring and Phe149 and Pro156. As an adenosine ring is present in the structure of Rio1 from the preparation to which no ATP was added, it is not surprising that there is no difference in the conformation of this flap in the three structures reported here.

Rio1 binds ATP in a unique conformation when compared with ePKs

As observed in other protein kinases, the ATP or ADP molecules in the Rio1–nucleotide–Mn complexes are bound between the N-lobe and the C-lobe and are contacted by the hinge region, the P-loop, the metal-binding loop, the catalytic loop, and Lys80 of the Rio1 kinase domain (Fig. 4A,B). The adenosine base participates in two hydrogen bonds with the hinge region, one from the peptide carbonyl oxygen of conserved Glu148 to the amino group N6, and one from the peptide amine of Ile150 to the indole nitrogen N1. The ribose moiety is contacted through water-mediated hydrogen bonds from the 2' hydroxyl to Glu162 and 3' hydroxyl to the backbone carbonyl oxygen of conserved Tyr200 (not shown). The triphosphate group is held in place by several contacts with conserved residues (Fig. 4B). The P-loop interacts through three water-mediated hydrogen bonds, between the hydroxyl side chain of conserved Ser56 and one of the β -phosphate oxygens, between the backbone amine of conserved Lys59 to the oxygen bridging the β - and γ -phosphate, and between the side-chain carboxylate of conserved Glu81 to one of the γ -phosphate oxygens. The Mn^{2+} ion coordinates oxygens from the β - and α -phosphates, the carbonyl oxygen of the catalytic loop residue Asn201, and a carboxyl oxygen from the metal-binding loop residue Asp212, along with two water molecules (Fig. 4B). Additional contacts with the triphosphates are made through the side chain amino group of Lys80 (conserved in all protein kinases) to α - and γ -phosphate oxygens, through a direct hydrogen bond between a carboxyl oxygen of the side chain of Asp212 and a γ -phosphate oxygen and, interestingly, through a water-mediated interaction between the indole nitrogen of Trp116 from the end of helix α C and a γ -phosphate oxygen (Fig. 4B). In the ADP complex, a water molecule replaces the γ -phosphate, but no significant conformational changes are observed in the active site (Fig. 4A).

Although the adenosine ring is buried deeper in Rio1 than in Rio2 proteins, the γ -phosphate is significantly more accessible. In the structure of Rio2 bound to ATP and Mn^{2+} , the γ -phosphate is buried through the ordering and binding of three residues of the N-terminal end of the flexible loop [21]. The P-loops of Rio1 and Rio2 are in different positions relative to the γ -phosphate, closer in the latter than in the former (Fig. 4C). The γ -phosphate is also more tightly bound in Rio2, where a second metal ion is seen which coordinates the γ -phosphate, and each γ -phosphate oxygen participates in two interactions with the

protein. In the case of Rio1, no metal ion is seen contacting the γ -phosphate and one of the phosphate oxygens makes no interactions with the protein. It is therefore conceivable that release of the γ -phosphate may be more difficult in Rio2 than Rio1, or may require further rearrangement of the Rio2 molecule. ATP interacts with the active site of Rio1 in a conformation similar to that seen in the Rio2-ATP complex (Fig. 4C). Only one Mn^{2+} ion was visible in the electron density (as opposed to two in the Rio2 complex). This ion superimposes exactly on one of the two Mn^{2+} ions of the Rio2-ATP complex when the protein chains of the two proteins are aligned. The same positioning of the Mn^{2+} ion is observed in the ADP complex.

However, this conformation is unique when compared with ePKs, such as serine/threonine kinases PKA (cyclic-AMP-dependent protein kinase) and CK (casein kinase), or the insulin receptor tyrosine kinase IRK [22–24]. The difference in position of the γ -phosphate results in a difference in the distance between the catalytic aspartate residue and the γ -phosphate (Fig. 4D). In PKA, this distance is 3.8 Å, while in Rio2 an equivalent distance is 5.8 Å. In the structure of Rio1 presented here, the distance between Asp196 and the nearest γ -phosphate oxygen is 5.1 Å. It should be noted that in IRK, this distance is also 5.8 Å for a complex with AMPPNP. Another significant difference between PKA and RIO kinases is the presence of an ePK conserved lysine from the catalytic loop of PKA (Lys168) which interacts with the γ -phosphate and is not seen in tyrosine kinases. This residue is replaced by a serine in all Rio1 kinases and by serine or aspartic acid in all Rio2 kinases, and the γ -phosphate is not located near it, as seen in Fig. 4D. Combined, these data suggest that the mechanism by which the catalytic aspartate of RIO kinases participates in phosphoryl transfer may be different than in known serine/threonine ePKs.

Conformational changes occur in Rio1 upon binding of nucleotides

Alignment of the C-lobe of the Rio1-ATP-Mn complex with that of the APO-Rio1 structure (RMSD = 0.58 Å, residues 157–257) shows a movement of the N-terminal domain relative to the C-terminal domain, with the nucleotide-binding P-loop moving closer to the active site (Fig. 3A). This rearrangement occurs through water-mediated contacts between the residues in the P-loop and the triphosphate moiety described above (Fig. 4B). The flexible loop, located between the end of helix α C and the start of β -strand 4, became

disordered on both ends. The entire ordered portion of the flexible loop, which contains a small helix in Rio1, repositions itself and forms new contacts (Fig. 2A). In addition, the catalytic loop and metal-binding loop are repositioned in the ATP-bound form. The catalytic loop between Leu192 and Leu197 is moved such that the α -carbon of Asp196 shifts by 1.48 Å towards the center of the active site cavity (Fig. 3A). The metal-binding loop between Phe210 and Ala216 moves towards the flexible loop, the α -carbon of Asp212 moves 0.87 Å and that of Gln215 moves 2.03 Å (Fig. 3A). None of these movements can be explained by differences in crystal contacts, as all four molecules in the asymmetric unit of the ATP complex are structurally identical in the regions for which the movement is described (Fig. 3C). This result indicates that Rio1 undergoes significant conformational changes in response to ATP binding, not only in the repositioning of one lobe relative to the other, but also in the movement of loops necessary for metal binding and catalysis. These conformational changes cannot be attributed to the presence of the γ -phosphate or to autophosphorylation, because the conformation of the protein in the presence of ADP and Mn^{2+} ions is essentially identical to that of the ATP complex. Therefore, the induction of conformational changes seen in these structures may rely solely on the presence of the diphosphate, or the metal ion, or both.

Rio1 autophosphorylates its flexible loop

In order to determine the site of autophosphorylation in AfRio1, we incubated the purified enzyme with γ - ^{32}P -labeled ATP and subjected the radiolabeled protein to phosphoamino acid analysis, as well as phosphopeptide mapping and sequencing. As shown in Fig. 5A, phosphoamino acid analysis of autophosphorylated AfRio1 showed that only phosphoserine is present. Digestion of the protein with trypsin and subsequent analysis of peptide fractions separated by HPLC showed only one radioactive peak, suggesting a single phosphorylated peptide (Fig. 5B). When this peptide was subjected to Edman degradation, ^{32}P was released at cycle 3 (Fig. 5C). When a similar procedure was applied to radiolabeled AfRio1 subjected to Asp-N and Glu-C proteolysis, the radioactive amino-acid was released at cycle 6 and cycle 8, respectively (Fig. 5D,E). An examination of the Rio1 sequence reveals that only labeling of Ser108 could result in the peptides consistent with the results given above. Ser108 is located at the end of the flexible loop, close to the start of helix α C. The observed autophosphorylation site is in good agreement with the prediction made

using the server NetPhos 2.0 (<http://www.cbs.dtu.dk>), which assigned a score of 0.998 to this site, with the next three highest scores being 0.891, 0.851 and 0.817.

In order to confirm this finding, we tested autophosphorylation activity of a mutant of Rio1 in which Ser108 was replaced by alanine (S108A). As predicted, the S108A mutant was incapable of autophosphorylation (Fig. 5F), yet it was able to phosphorylate histone H1 and myelin basic protein as efficiently as the wild-type Rio1 (Fig. 5G). A second mutant, D196A, in which the putative catalytic aspartate was replaced by alanine showed drastic reduction in activity, confirming that this residue is indeed important for the catalytic activity of the Rio1 proteins (Fig. 5F,G). In the presence of the S108A mutant, the D196A protein is phosphorylated to the level similar to that of the autophosphorylated wild-type Rio1 (Fig. 5F). Combined, these data confirm that Ser108 is the sole site for autophosphorylation of AfRio1, and indicate that phosphorylation of the Rio1 protein is not necessary for the maintenance of the kinase activity using the substrates that were tested.

In addition, we compared the levels of autophosphorylation observed using the *A. fulgidus* Rio1 protein with that obtained using *A. fulgidus* Rio2. We incubated equivalent amounts of each protein with radiolabeled ATP or GTP and magnesium ions at the same concentration. The resulting autoradiograph is shown in Fig. 5H. Based on comparison of the bands for Rio1 in the presence of ATP and that for Rio2, Rio1 appears to be more active at autophosphorylation than Rio2 and both enzymes preferred ATP to GTP.

Rio1-specific conserved residues

A number of residues are specifically conserved in the Rio1 subfamily and they lend several distinguishing characteristics to the Rio1 kinase domain. The presence of the Rio1-specific helices α 1 and α 2, located N-terminal to the RIO domain, appears to be a conserved feature of Rio1 proteins based on their sequence alignments. It is now clear that the distinct P-loop sequence GxxSTGKEANVY/F of the Rio1 proteins is designed to accommodate several differences in ATP binding between Rio1 and Rio2 (the latter contains a P-loop with the sequence xxxGxGKESxVY/F). Invariant Ser56 of the Rio1 P-loop participates in a water-mediated interaction with the β -phosphate of the ATP. In Rio2, an equivalent residue is a glycine, and the β -phosphate is instead contacted directly by the invariant Ser104 of the P-loop (Fig. 4A,C). In Rio1, the invariant Ala61 of the P-loop is necessary because of the specific

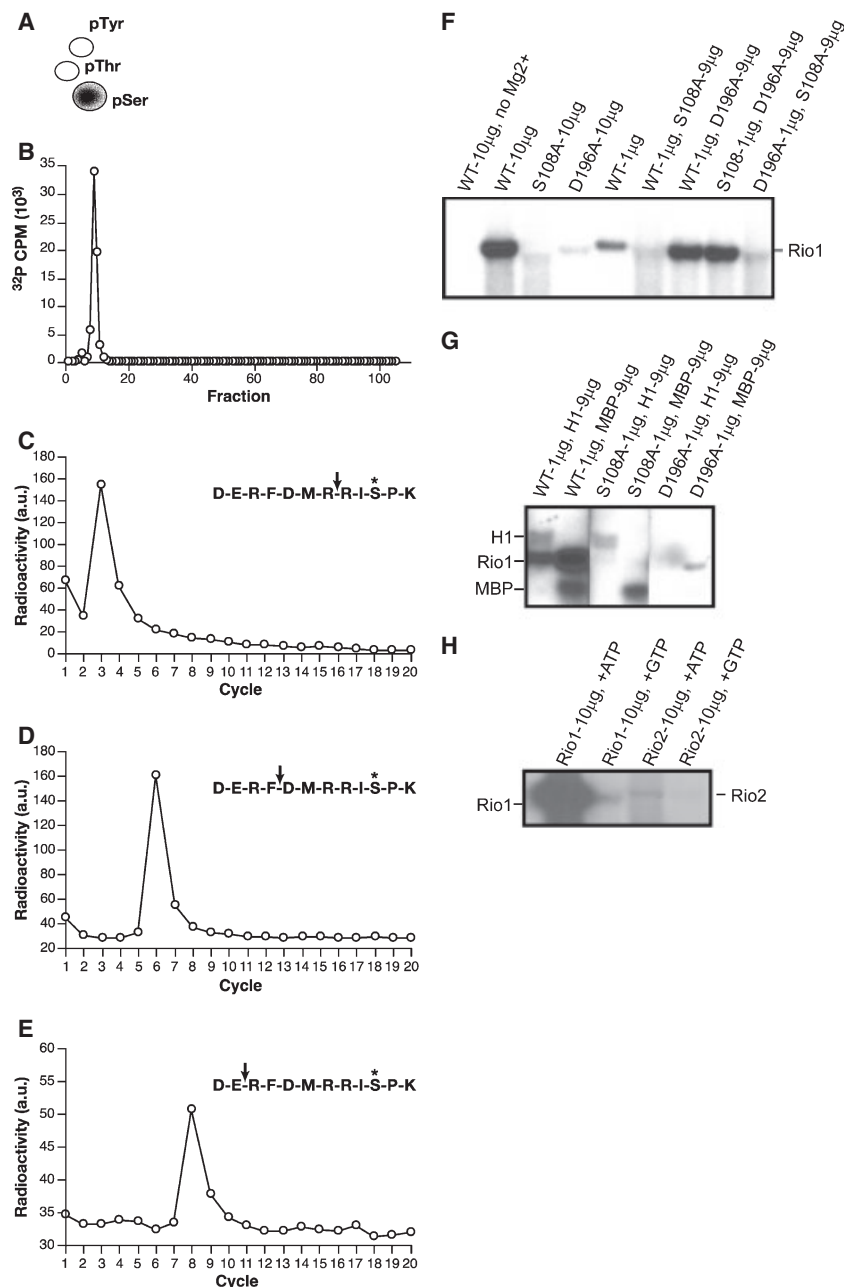


Fig. 5. Rio1 is autophosphorylated within the flexible loop. (A) Phosphoamino acid analysis of autophosphorylated AfRio1. (B) Radioactivity levels of fractions from reverse-phase HPLC separation of the tryptic peptides from autophosphorylated AfRio1. (C–E) Edman degradation of peptides obtained from the radioactive fraction of HPLC separation of proteolytic digests of autophosphorylated Rio1 using (C) trypsin, (D) Glu-C and (E) Asp-N. Inserted text shows sequence surrounding calculated phosphorylation site with an arrow to indicate cleavage site for each enzyme. (F) Autophosphorylation activity of Rio1 wild-type (WT) and Rio1 mutant proteins (S108A, D196A) incubated with γ - 32 P-labeled ATP. Amounts of each protein in the reaction are indicated in the labels. (G) Phosphorylation activity of wild-type and mutant Rio1 on common kinase substrate histone H1 (H1) and myelin basic protein (MBP). (H) Autophosphorylation activity of equivalent amounts of AfRio1 and AfRio2 in the presence of ATP and GTP.

conservation of residues at the end of strand β 3. This region is highly conserved in both Rio1 and Rio2 proteins, although the sequence is different between the two subfamilies (Fig. 1D). The invariant Tyr82 of this sequence is involved in positioning of the metal-binding Asp212 and its side chain aromatic ring located very near Ala61 (3.91 Å between the alanine C β and the nearest aromatic carbon) in the presence of ATP or ADP (Fig. 4A,B). As such, a longer polar side chain would not be accommodated in the position of

Ala61. Tyr82 is replaced by His122 in Rio2 proteins, which therefore can accommodate a Ser in the position equivalent to Rio1 Ala61 (Fig. 4C). Asn62 appears to play a role in conformational changes in response to nucleotide binding. In the absence of a nucleotide, the side chain of Asn66 hydrogen bonds with the conserved Arg83 at the end of β 3. Arg83 also hydrogen bonds to the carbonyl oxygen of Gly58 in the P-loop. Asn62 and Arg83 do not interact in the presence of a nucleotide and the side chain of Arg83 is in that case

repositioned to form a hydrogen bond with the carbonyl oxygen of Lys59 (data not shown).

Some of the conserved residues are required for the formation of the flexible loop and its binding surface on Rio1. These residues are involved in hydrophobic packing interactions, hydrogen bond interactions, and interactions that change in response to nucleotide binding. These include the YL and RF motifs from the flexible loop (Fig. 1D), the Trp116, Lys119, Arg122 and Asn123 from α C, Gln215 of the catalytic loop and the HP motif between β 10 and α F. All these residues, except for Gln215, are specifically conserved in the Rio1 subfamily, which suggests a subfamily

specific conformation of the flexible loop in RIO proteins.

Some of the conserved residues are located on the surface of the molecule and are not involved in intramolecular interactions. They include Phe89 within the flexible loop, Glu199 and Tyr200 within the catalytic loop, and Lys59 in the P-loop. These residues are clustered around the active site, and therefore may be involved in interactions with the substrate. When the conserved residues are mapped to the surface, it appears that they cluster mainly around the active site and around the flexible loop binding site (Fig. 6A). A large conserved area which may be the site of substrate

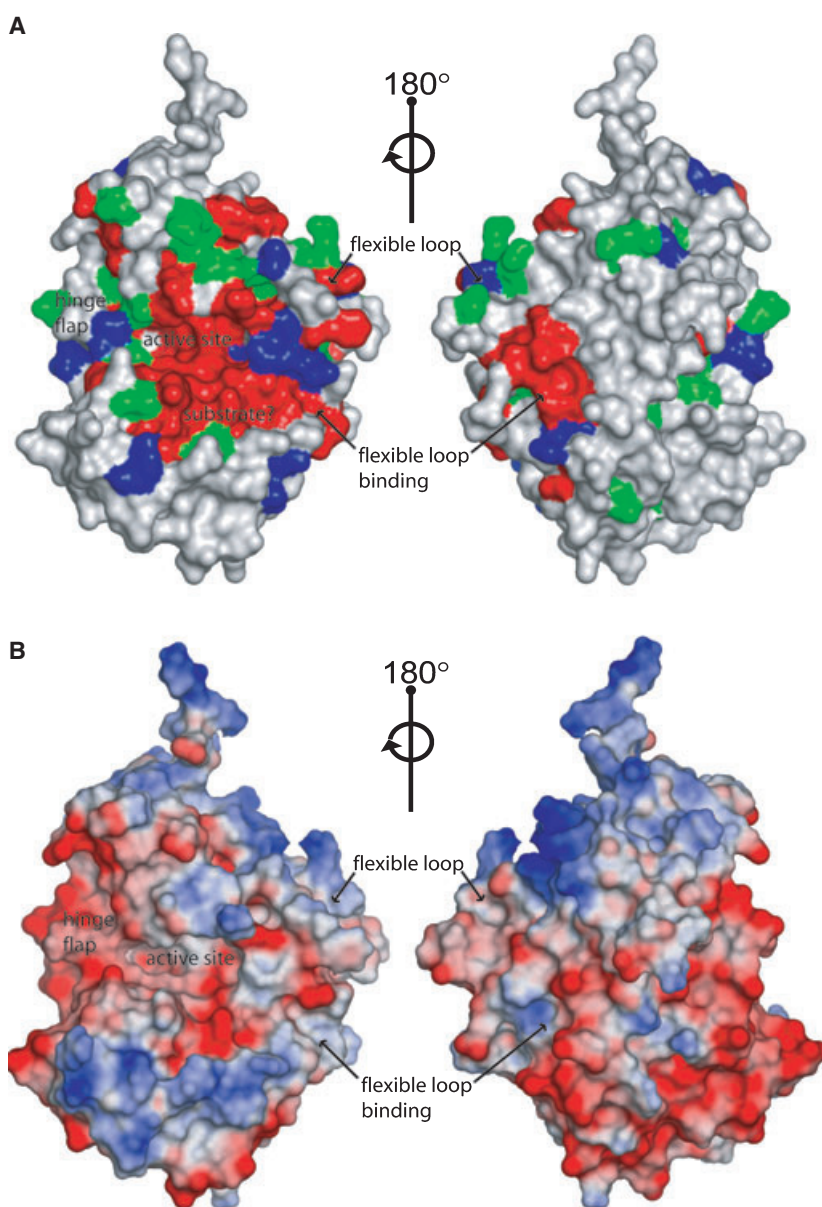


Fig. 6. Location of the conserved residues of the Rio1 protein. (A) Conserved residues of the Rio1 protein mapped to the protein surface. Red = identical, green = highly conserved, blue = weakly similar, and white = not conserved. (B) Electrostatic surface of the Rio1 protein (red = negative, blue = positive).

binding is present in the C-lobe outside the active site. Analysis of the electrostatic surface in this region shows a largely negatively charged surface surrounding the active site, with some small nonpolar patches (Fig. 6C). The presence of basic residues within the autophosphorylation site sequence, DMRRISPKEK, would agree with the presence of negative charge surrounding the active site. However, as the Rio1 kinase is so divergent from the ePKs for which the structures with bound substrates are known, at present we are unable to model the position of the substrate peptide.

Discussion

Determination of the structure of AfRio1 and its comparison with the structure of AfRio2 has allowed us to define the minimal extent of a RIO domain. The previously determined structure of Rio2 has indicated that the RIO domain was a truncated version of the ePK catalytic domain, lacking several important loops known to interact with peptide substrate, namely subdomains VIII, X and XI. However, comparison of the two structures has shown that the RIO domains contain an additional helix N-terminal to the β -sheet of the N-lobe that packs on top of it (α R in Fig. 1A, B, D). This extension, originally described as part of the winged-helix N-terminal domain of Rio2, is not a conserved part of canonical ePK kinase domain, but appears to be a feature of the RIO kinases. The Rio1 structure has also enabled us to define the flexible loop as an enduring feature of RIO domains. This insertion is present in all the RIO subfamilies, and contains subfamily conserved sequences, indicating a specific function for each subfamily.

In addition to defining the conserved structural features between the RIO subfamilies, these structures have highlighted the important differences between the Rio1 and Rio2 proteins. The differences between conserved residues in the P-loop (STGKEA in Rio1 and GxGKES in Rio2) and the end of β 3 (AV/IKIY in Rio1 and (vVKFHK/R) appear to be directly related to how Rio1 and Rio2 interact with the triphosphate moiety of ATP. As a result of the changes, the triphosphate group is contacted by water-mediated interactions from the P-loop in Rio1, as opposed to direct interactions in Rio2. In addition, the γ -phosphate in Rio1 is more accessible than in Rio2, due to interactions between Rio2 and the beginning of the flexible loop. The difference in the length of the hinge region between Rio1 and Rio2 is due to an insertion of a β -hairpin in Rio1 that closes off the active site. This produces a deeper ATP binding pocket in the Rio1 proteins which may translate to differences in

kinase activity. The differences in the conserved residues of the flexible loop and the important helix α C directly relate to the interactions between the Rio1 flexible loop and α C, and the conformational changes that occur in the Rio1 protein in response to ATP binding.

Several important differences between the way Rio1 and Rio2 respond to nucleotide binding should be pointed out. Although the N-lobe moves relative to the C-lobe when Rio2 binds ATP, the catalytic loop and the metal-binding loop do not shift significantly. By contrast, significant conformational changes that include the catalytic loop, the metal-binding loop, and the flexible loop are seen in Rio1. Overall, the differences between the two subfamilies suggest a difference in the strength of binding of nucleotides to Rio1 and Rio2. Indeed, this is highlighted by the fact that Rio1 retained the adenosine molecule through all steps of purification, whereas Rio2 did not. In addition, the comparison of Rio1 to Rio2 suggests a probable difference in the rate of phosphoryl transfer. The accessibility of the γ -phosphate in Rio1 indicates that in the conformation observed in the crystal, the protein may be ready to accept substrate. However, the lack of accessibility of the γ -phosphate in Rio2 suggests a requirement for additional conformational changes or activation. The γ -phosphate is located closer to the catalytic aspartate residue in Rio1 (5.1 Å) than in Rio2 (5.8 Å). We have observed a dramatic difference in the autophosphorylation activity of the protein, with AfRio1 being far more active than AfRio2 (Fig. 5H).

The flexible loop is an interesting feature of the Rio1 kinase. The dynamic nature of this region is apparent in the movement of the entire loop when nucleotide binds, affecting changes in interactions with residues near the γ -phosphate. A conserved Gln residue (Gln215) is found four residues N-terminal to the metal-binding Asp residue in all RIO kinases. However, in Rio1, in the absence of nucleotide, its side chain hydrogen bonds to a conserved residue (Tyr95) present in the flexible loop (Fig. 3B). When ATP and Mn^{2+} are bound, this glutamine moves to contact one of the carboxyl oxygens of the metal-binding Asp212. The switching of the positions of Trp116 and Met92 in response to nucleotide binding also results in the movement of Tyr82 towards the γ -phosphate. These and other movements indicate that the flexible loop may play an important role in the interactions with nucleotide and substrate. Although it was observed that autophosphorylation detected in this region does not appear to be necessary for kinase activity, we cannot rule out regulatory effects through interaction with

other proteins, and thus a regulatory role for the flexible loop remains a possibility.

Autophosphorylation has been observed in all RIO kinases studied thus far, but the importance of this activity has not yet been determined. The sole autophosphorylation site of AfRio1 was identified as Ser108, which is located within the flexible loop region that becomes disordered when a nucleotide is bound. We have determined that the phosphorylation state of that serine is not directly related to the order or disorder of this region, as the structure of Rio1 in crystals grown with only ADP and Mn present, incapable of autophosphorylation, display disorder in these regions as well. We have additionally shown that the S108A mutant, although incapable of autophosphorylation, still exhibits kinase activity comparable to the wild-type protein. This result indicates that autophosphorylation is not necessary for this activity. This serine is not conserved in Rio1 proteins, and this site may be specific to *A. fulgidus* Rio1. Although this particular serine is not conserved, Rio1 from other species contain a conserved K/RTS motif directly adjacent to the conserved portion of β 3 which may replace this autophosphorylation site (Fig. 1D). This is analogous to the autophosphorylation site determined for AfRio2 on Ser128, also located near the end of β 3, directly adjacent to a portion of the flexible loop that becomes ordered in the presence of ATP [21]. Although a TS sequence is present in a similar position in AfRio1, the residue preceding it is a Glu, which may be unfavorable for substrate binding given the largely positively charged surface outside of the catalytic site (Figs 1D and 6D). The site(s) of autophosphorylation in eukaryotic Rio1 proteins still remain to be identified.

The structure presented here has confirmed that ATP assumes a conformation in complexes with the RIO kinases that is different in comparison to its conformations in known ePKs. The triphosphate moiety of the ATP molecule in PKA and other ePKs is normally bent by the coordination of both the α - and γ -phosphates by a single metal ion. In both Rio1 and Rio2, the triphosphate moiety is found in an extended conformation. When such a conformation was first observed in AfRio2 where two metal ions are bound instead of one, it was not entirely clear that it represented productive binding. However, as it has now been seen in both Rio1 and Rio2, it is more likely that it is not an artifact. If this is indeed the case, we now need to explain how the catalytic Asp, thought to act as a catalytic base in Ser/Thr ePKs, contributes to catalysis, given the large distance between its side chain and the γ -phosphate in both Rio1 and Rio2. It

is clear that this residue does play an important role in Rio1, as mutation of Asp196 to Ala leads to drastically decreased catalytic activity. The presence of one metal ion between the β - and α -phosphate in the Rio1 structure is unusual, as the metal ion is typically coordinated to the phosphate which is to be transferred. It is thus plausible that an additional binding site, in a position similar to the one seen in Rio2 between the β - and γ -phosphate, may exist but not be occupied in the crystal structure presented here because of partial occupancy of the γ -phosphate, or lack of substrate interactions. In any case, because of the altered position of the γ -phosphate, we believe that phosphoryl transfer, as well as substrate binding, may be significantly different in Rio1 than in canonical Ser/Thr ePKs. However, a structure with the substrate is required to determine the final position of the γ -phosphate, the serine hydroxyl group, and the catalytic Asp prior to phosphoryl transfer.

The large differences between RIO kinases and ePKs, coupled with the lack of protein substrate in the structures of the former enzymes, make it impossible at this time to present detailed models of substrate binding in the Rio1 kinases. Analysis of the conserved surface residues shows their clustering around the active site, and the electrostatic surface analysis shows a negatively charged region surrounding the active site (Fig. 6). This would be consistent with the presence of two basic residues, Arg105 and Arg106, N-terminal to the determined autophosphorylation site. Studies are underway to determine whether a peptide substrate can be phosphorylated by the Rio1 kinase. As this enzyme lacks the loops which bind substrate peptide in ePKs and as the conserved residues are spread over a large area surrounding the active site, our first thought was that RIO kinases may not interact with peptides, but rather with whole protein surfaces. However, Rio1 and Rio2 kinases each autophosphorylate a residue located in the flexible loop, and in the case of Rio2 the site is conserved, indicating that RIO proteins may indeed recognize specific peptide substrates.

These structures have provided the molecular detail necessary to probe the function of the Rio1 kinase in ribosome biogenesis. They have also provided information that shows a clear distinction between the Rio1 and Rio2 subfamilies, as well as between RIO kinases and canonical ePKs. Involvement of these enzymes in ribosome biogenesis makes them both attractive targets for inhibition. Based on the unique features in the active sites of these enzymes, it is conceivable that inhibitors could be designed that are RIO kinase specific, as well as RIO subfamily specific.

Experimental procedures

Protein expression and purification

The full-length Rio1 gene was PCR amplified from *A. fulgidus* genomic DNA (ATCC) and subcloned into a plasmid vector containing an N-terminal His₆ tag followed by a Tobacco Etch Virus (TEV) protease cleavage site (Protein Expression Laboratory, SAIC, Frederick, MD, USA). This construct was transformed into *E. coli* RosettaTM-DE3-pLysS cells (Novagen, Madison, WI, USA). Expression cultures were grown at 37 °C and induced with 1 mM isopropyl thio-β-D-galactoside at $D_{600} = 0.6$ for 4 h. After expression, the cells were harvested by centrifugation and resuspended in 50 mL of 50 mM Tris pH 8.0, 100 mM NaCl, 0.2 X Bugbuster (Novagen) and 0.1 mg·mL⁻¹ DNaseI (Roche, Indianapolis, IN, USA) per litre of expression culture and stirred at room temperature. After 20 min, the lysate was transferred to centrifuge tubes and placed in a 75 °C water bath for 15 min to denature the *E. coli* proteins then immediately centrifuged for 20 min at 16 000 r.p.m. in a Beckman SS-34 rotor to remove insoluble material. The supernatant, which contained the thermostable Rio1, was diluted two-fold with purified water, passed through a 0.22 μm filter and loaded onto a 5 mL HisTrap HP column (APBiotec, Piscataway, NJ, USA) equilibrated in buffer containing 50 mM Tris pH 8.0 and 100 mM NaCl (equilibration buffer). The bound Rio1 was washed in 100 mM imidazole in equilibration buffer and then eluted with 400 mM imidazole in equilibration buffer. The fractions containing Rio1 were pooled and equilibration buffer containing 2 mM EDTA and 0.4% (v/v) 2-mercaptoethanol was used to dilute the pooled fractions twofold. The resulting mixture was placed in dialysis membrane to which TEV protease was added to 20 μg·mL⁻¹. The protein was dialyzed over-night at room temperature into 50 mM NaCl, 25 mM Tris pH 8.0, 1 mM EDTA and 0.2% (v/v) 2-mercaptoethanol. The dialysate was loaded onto a 5 mL HiTrap Blue column (APBiotec) equilibrated in 50 mM NaCl, 25 mM Tris pH 8.0, 1 mM EDTA. The protein was eluted in a gradient from 0.050 to 3 M NaCl in 20 column volumes. The ~98% pure protein was further purified to > 99% purity by size exclusion chromatography using a column packed with Superdex 75 resin (APBiotec) equilibrated in 20 mM Tris pH 7.5 and 200 mM NaCl. The buffer was exchanged to 10 mM Tris pH 8.0, 10 mM NaCl, 1 mM EDTA by several rounds of dilution and concentration. The concentration of the final protein solution was 20 mg·mL⁻¹. This preparation was stored at room temperature until crystallization screening. Se-Met Rio1 was expressed in minimal media with all amino acids supplemented except for methionine, which was replaced by Se-Met. Reducing agent [0.2% (v/v) 2-mercaptoethanol] was added to Se-Met protein immediately prior to crystallization screening.

Radiolabeling of AfRio1

In order to produce radiolabeled Rio1 to determine its autophosphorylation site(s), the enzyme was incubated for 60 min at 37 °C in the presence of ³²P-labeled ATP. The reaction buffer contained 50 mM NaCl, 50 mM Tris pH 7.5 and 20 μCi [³²P]ATP[γP] with 2 mM MgCl₂. All reactions for radiolabeling contained 150 μg of the enzyme in 30 μL total reaction volume. Half of the reaction mixtures were run in each lane (30 μg of protein) of a NuPAGE 4–12% Bis-Tris denaturing gel (Invitrogen, Carlsbad, CA, USA) for 1 h at 120 V. The labeled protein was then transferred onto Invitrolon P membrane using Xcell Blot II apparatus (both Invitrogen) according to the manufacturer's instructions. The resulting membrane was used to expose a film for 10 min to determine the position of the labeled bands, and the bands were cut out for phosphoamino acid analysis and phosphopeptide mapping and sequencing.

Phosphoamino acid analysis

A portion of the membrane was hydrolyzed in 200 μL 4 M HCl at 110 °C for 1.5 h. Phosphoamino acid standards were added and the solution was lyophilized. The contents were redissolved in electrophoresis buffer (acetic acid/formic acid/water, 15 : 5 : 80, v/v/v) and applied to 20 × 20 cm cellulose TLC plates. The plate was electrophoresed at 1500 V for 40 min then rotated 90° and subjected to chromatography overnight using 0.5 M NH₄OH/isobutyric acid, 3 : 5, v/v. The plate was dried and sprayed with ninhydrin to localize the phosphoamino acid standards. Radioactivity was detected and visualized with a Typhoon Model 9200 phosphoimager (Amersham Biosciences, Little Chalfont, Bucks, UK).

Phosphopeptide mapping

The membrane was cut into small pieces and washed sequentially with methanol, distilled water and then blocked with 1.5% poly(vinylpyrrolidone)-40 in 100 mM acetic acid. Membranes were digested with either trypsin, or Glu-C proteases in 50 mM NH₄HCO₃ pH 8 overnight, or with Asp-N protease in 50 mM sodium phosphate pH 8 overnight. All enzymes were purchased from Roche. Supernatants containing released peptides were removed, adjusted to pH 2 with 20% aqueous trifluoroacetic acid and subjected to reversed phase HPLC on a Waters 3.9 × 300 mm C₁₈ column. The column was developed with a gradient of 0–30% (v/v) acetonitrile in 0.05% (v/v) aqueous trifluoroacetic acid over 90 min at a flow rate of 1 mL·min⁻¹. One milliliter fractions were collected and counted for ³²P in a Beckman 6500 scintillation counter [25]. ³²P peptides were coupled to Sequalon disks and subjected to solid phase Edman degradation with a Model 492 Applied Biosystems peptide sequencer. Cycle fractions were collected onto Water #1 paper discs and

radioactivity was quantitated using a Typhoon (Molecular Dynamics, Sunnyvale, CA, USA) phosphoimager.

Kinase assays

To produce mutant Rio1 proteins, site directed mutants were made using the QuikChange™ Site-directed Mutagenesis kit (Stratagene, La Jolla, CA, USA) with the AfRio1 expression vector described above as a template. The mutants were expressed and purified as described above for the wild-type protein. All assays were performed in 20 μ L reaction volumes containing 25 mM Tris pH 7.5, 50 mM NaCl and 2 mM MgCl₂. In the control reaction containing no magnesium ions, 25 mM EDTA was added to the reaction to remove trace divalent cations. The amounts of kinase (1 or 10 μ g) and protein substrates (9 μ g) in the reactions are as indicated in Fig. 6. All components were mixed prior to the addition of 5 μ Ci of γ -³²P-labeled ATP. Histone H1 (Roche) and myelin basic protein (MBP, Sigma-Aldrich, St Louis, MO, USA) were used as protein substrates. In the comparison of Rio1 and Rio2 in Fig. 6C, 10 μ Ci of either γ -³²P-labeled ATP or γ -³²P-labeled GTP was used. The reaction mixtures were incubated at 37 °C for 1 h and run on a NuPAGE 4–12% Bis-Tris denaturing gel (Invitrogen) for 1 h at 150 V. The gel was then dried and used to expose film for 5–30 min.

Crystallization

Initial crystallization conditions were obtained through utilization of several sparse matrix screens (Emerald Biostructures Inc., Bainbridge Island, WA, USA; Nextal, Montreal, Quebec, Canada; Hampton Research, Aliso Viejo, CA, USA) with the hanging drop vapor diffusion method. Crystals of the Rio1 protein in the absence of nucleotide were obtained from drops consisting of a mixture of equal volumes of protein and well solution, containing 16–26% polyethylene glycol (PEG) 4000, 100 mM MES buffer pH 6.0–6.5 and 200 mM ammonium sulfate placed over 1 mL reservoirs. Diffraction quality crystals (300–500 \times 300 \times 5 μ m in size) were obtained after 4 days at 20 °C. Crystals of Rio1 grown in the presence of ATP were obtained in the same conditions using protein solutions to which 20 mM ATP and 20 mM MnCl₂ had been added. Diffraction quality crystals of similar morphology were observed after 2 weeks. However, streak seeding produced crystals of adequate size after 4 days.

Data collection and processing

Se-Met crystals, ADP- and ATP-containing crystals were flash frozen in mother liquor containing 15% (v/v) glycerol. Diffraction data for the nucleotide free, Se-Met and ATP crystals were collected at 100 K at the SER-CAT

beamline at the Advanced Photon Source (APS), Argonne, IL, USA. Data from the Se-Met crystals were collected at three wavelengths (peak, inflection point, and remote). As the space group is monoclinic, 360° of data were collected at each wavelength in 90° inverse wedges to maximize redundancy. All data were integrated and merged using HKL2000 [26]. Table 1 contains details regarding data statistics for all data sets.

Structure determination and refinement

The AUTOSHARP program suite was used for the Se-Met data set to obtain the phases using the MAD method, apply solvent flattening and density modification to the initial electron density map, and perform automatic model building with WARP [27]. The complete model was finalized by rebuilding in XTALVIEW [28] and refinement with REFMAC5 [29]. The completely refined model was used as a molecular replacement model to phase the ADP-Mn and ATP-Mn-containing data sets using MOLREP as part of CCP4i [30]. These models were subjected to several rounds of building in XTALVIEW and refinement using REFMAC5. R_{free} was monitored by using 5% of the reflections as a test set in each case. Refinement statistics are provided in Table 1. The coordinates and structure factors have been deposited in the Protein Data Bank (accession codes 1ZTF for the APO, 1ZP9 for the ATP-Mn-bound and 1ZTH for ADP-bound enzyme).

Acknowledgements

We would like to express our gratitude to Dr Zbyszek Dauter for help in collecting and analyzing the crystallographic data utilized in this study and to Dr Sook Lee and Dr Peter Johnson for assistance with kinase assays. Diffraction data were collected at the South-East Regional Collaborative Access Team (SER-CAT) beamline 22-ID, located at the Advanced Photon Source, Argonne National Laboratory. Use of the Advanced Photon Source was supported by the U. S. Department of Energy, Office of Science, Office of Basic Energy Sciences, under Contract No. W-31-109-Eng38.

References

- 1 Moss T (2004) At the crossroads of growth control; making ribosomal RNA. *Curr Opin Genet Dev* **14**, 210–217.
- 2 Comai L (1999) The nucleolus: a paradigm for cell proliferation and aging. *Braz J Med Biol Res* **32**, 1473–1478.
- 3 Ruggero D & Pandolfi PP (2003) Does the ribosome translate cancer? *Nat Rev Cancer* **3**, 179–192.

- 4 Tere D, Ceccarelli C, Montanaro L, Tosti E & Derenzini M (2004) Nucleolar size and activity are related to pRb and p53 status in human breast cancer. *J Histochem Cytochem* **52**, 1601–1607.
- 5 Granneman S & Baserga SJ (2004) Ribosome biogenesis: of knobs and RNA processing. *Exp Cell Res* **296**, 43–50.
- 6 Manning G, Whyte DB, Martinez R, Hunter T & Sudarsanam S (2002) The protein kinase complement of the human genome. *Science* **298**, 1912–1934.
- 7 Hanks SK & Hunter T (1995) Protein kinases 6: the eukaryotic protein kinase superfamily: kinase (catalytic) domain structure and classification. *FASEB J* **9**, 576–596.
- 8 Bossemeyer D (1995) Protein kinases – structure and function. *FEBS Lett* **369**, 57–61.
- 9 Engh RA & Bossemeyer D (2002) Structural aspects of protein kinase control-role of conformational flexibility. *Pharmacol Ther* **93**, 99–111.
- 10 Hanks SK, Quinn AM & Hunter T (1988) The protein kinase family: conserved features and deduced phylogeny of the catalytic domains. *Science* **241**, 42–52.
- 11 Knighton DR, Zheng JH, Ten Eyck LF, Ashford VA, Xuong NH, Taylor SS & Sowadski JM (1991) Crystal structure of the catalytic subunit of cyclic adenosine monophosphate-dependent protein kinase. *Science* **253**, 407–414.
- 12 Knighton DR, Zheng JH, Ten Eyck LF, Xuong NH, Taylor SS & Sowadski JM (1991) Structure of a peptide inhibitor bound to the catalytic subunit of cyclic adenosine monophosphate-dependent protein kinase. *Science* **253**, 414–420.
- 13 Leonard CJ, Aravind L & Koonin EV (1998) Novel families of putative protein kinases in bacteria and archaea: evolution of the ‘eukaryotic’ protein kinase superfamily. *Genome Res* **8**, 1038–1047.
- 14 Angermayr M, Roidl A & Bandlow W (2002) Yeast Rio1p is the founding member of a novel subfamily of protein serine kinases involved in the control of cell cycle progression. *Mol Microbiol* **44**, 309–324.
- 15 Angermayr M & Bandlow W (2002) RIO1, an extraordinary novel protein kinase. *FEBS Lett* **524**, 31–36.
- 16 Vanrobays E, Gleizes PE, Bousquet-Antonelli C, Noaillac-Depeyre J, Caizergues-Ferrer M & Gelugne JP (2001) Processing of 20S pre-rRNA to 18S ribosomal RNA in yeast requires Rrp10p, an essential non-ribosomal cytoplasmic protein. *EMBO J* **20**, 4204–4213.
- 17 Vanrobays E, Gelugne JP, Gleizes PE & Caizergues-Ferrer M (2003) Late cytoplasmic maturation of the small ribosomal subunit requires RIO proteins in *Saccharomyces cerevisiae*. *Mol Cell Biol* **23**, 2083–2095.
- 18 Geerlings TH, Faber AW, Bister MD, Vos JC & Raue HA (2003) Rio2p, an evolutionarily conserved, low abundant protein kinase essential for processing of 20 S Pre-rRNA in *Saccharomyces cerevisiae*. *J Biol Chem* **278**, 22537–22545.
- 19 Giaever G, Chu AM, Ni L, Connelly C, Riles L, Veroneau S, Dow S, Lucau-Danila A, Anderson K, Andre B *et al.* (2002) Functional profiling of the *Saccharomyces cerevisiae* genome. *Nature* **418**, 387–391.
- 20 LaRonde-LeBlanc N & Wlodawer A (2004) Crystal structure of *A. fulgidus* Rio2 defines a new family of serine protein kinases. *Structure (Camb)* **12**, 1585–1594.
- 21 LaRonde-LeBlanc N, Guszczynski T, Copeland TD & Wlodawer A (2005) Autophosphorylation of *Archaeoglobus fulgidus* Rio2 and crystal structures of its nucleotide–metal ion complexes. *FEBS J* **272**, 2800–2811.
- 22 Zheng J, Knighton DR, Ten Eyck LF, Karlsson R, Xuong N, Taylor SS & Sowadski JM (1993) Crystal structure of the catalytic subunit of cAMP-dependent protein kinase complexed with MgATP and peptide inhibitor. *Biochemistry* **32**, 2154–2161.
- 23 Xu RM, Carmel G, Sweet RM, Kuret J & Cheng X (1995) Crystal structure of casein kinase-1, a phosphate-directed protein kinase. *EMBO J* **14**, 1015–1023.
- 24 Hubbard SR (1997) Crystal structure of the activated insulin receptor tyrosine kinase in complex with peptide substrate and ATP analog. *EMBO J* **16**, 5572–5581.
- 25 Morrison DK, Heidecker G, Rapp UR & Copeland TD (1993) Identification of the major phosphorylation sites of the Raf-1 kinase. *J Biol Chem* **268**, 17309–17316.
- 26 Otwinowski Z & Minor W (1997) Processing of X-ray diffraction data collected in oscillation mode. *Methods Enzymol* **276**, 307–326.
- 27 Perrakis A, Morris R & Lamzin VS (1999) Automated protein model building combined with iterative structure refinement. *Nat Struct Biol* **6**, 458–463.
- 28 McRee DE (1999) XtalView/Xfit – a versatile program for manipulating atomic coordinates and electron density. *J Struct Biol* **125**, 156–165.
- 29 Murshudov GN, Vagin AA & Dodson EJ (1997) Refinement of macromolecular structures by the maximum-likelihood method. *Acta Crystallogr* **D53**, 240–255.
- 30 Collaborative Computational Project Number 4 (1994) The CCP4 suite: programs for protein crystallography. *Acta Crystallogr* **D50**, 760–763.